PRODUCTION OF PIONS BY NEGATIVE PIONS ON HYDROGEN NEAR THE THRESHOLD

V. G. ZINOV and S. M. KORENCHENKO

Joint Institute for Nuclear Research

Submitted to JETP editor October 19, 1957

J. Exptl. Theoret. Phys. (U.S.S.R.) **34**, 301-311 (February, 1958)

Production of pions on hydrogen by 307, 333, and 370 Mev negative pions was studied with scintillation counters. In the processes $\pi^- + p \rightarrow \pi^- + \pi^+ + n$ and $\pi^- + p \rightarrow \pi^- + \pi^0 + p$, the differential cross-section for the formation of a charged meson at an angle of 80° in the laboratory system (106 deg in the c.m.s.) turns out to be $(0.10 \pm 0.06) \times 10^{-27}$, $(0.17 \pm 0.06) \times 10^{-27}$, and $(0.29 \pm 0.05) \times 10^{-7}$ cm^2/sterad for 307, 333, and 370 Mev π^- mesons respectively.

INTRODUCTION

THE production of pions by negative pions on hydrogen, an event that becomes energetically possible when the energy of the incident pion exceeds 170 Mev, has been studied to date only at high energies.[1] The study of the creation of pions by negative pions near the production threshold is of interest not alone from the theoretical point of view. Such measurements are also necessary to estimate the contribution of the creation processes to the experimentally-observed scattering cross-sections of pions.

In addition to causing the scattering processes

$$\pi^- + p \rightarrow \pi^- + p \text{ (elastic scattering)} \quad (1)$$

$$\pi^- + p \rightarrow \pi^0 + n \text{ (exchange scattering)} \quad (2)$$

$$\pi^0 \rightarrow 2\gamma$$

the interaction of negative pions with hydrogen may also result in the following creation processes:

$$\pi^- + p \rightarrow \pi^- + \pi^+ + n; \quad (3)$$

$$\pi^- + p \rightarrow \pi^- + \pi^0 + p; \quad (4)$$

$$\pi^- + p \rightarrow \pi^0 + \pi^0 + n. \quad (5)$$

The work reported here was performed for the purpose of estimating the cross-sections of processes (3) and (4) in the 300 — 370 Mev energy region. It turns out that for 307-Mev negative pions, the negatively charged mesons, produced on hydrogen and recorded at an angle of 80° in the laboratory system, comprise approximately 10% of the number of the elastically scattered negative pions, and the fraction rises to 40% for 370-Mev π^- mesons. Apparently, at 370 Mev, approximately 15% of the total interaction cross-section for the interaction of π^- mesons with hydrogen (i.e., 3.5 to 4 × 10^{-27} cm^2), is due to the creation of mesons by mesons.

BEAMS OF NEGATIVE PIONS, SCINTILLATION COUNTERS, AND ELECTRONIC APPARATUS

Beams of 250, 307, 333, and 370 Mev negative pions, obtained behind the armature of the magnet of the synchrocyclotron of the Joint Institute for Nuclear Research,[2,3] were used. The 250-Mev negative-pion beam was obtained from the 300-Mev beam by means of polyethylene absorbers. The energy of the negative-pion beams were determined from their range in copper. A typical absorption curve is shown in Fig. 1. The muon content in the 300 — 370 Mev beams was 5 ± 1.5%. The muon content of the 250-Mev beam was not determined. The intensities of the various beams were 45, 150, 100, and 45 mesons/cm^2-sec for the 250, 307, 333, and 370 Mev beams respectively.

The intensity distribution over the cross-section of the beam was studied for each beam energy with the aid of a 1×1×1 cm scintillator.

Scintillation counters were used to record the particles. The experimental geometry is shown in Fig. 2. Scintillation counters 1, 3, 4, 7, and 8

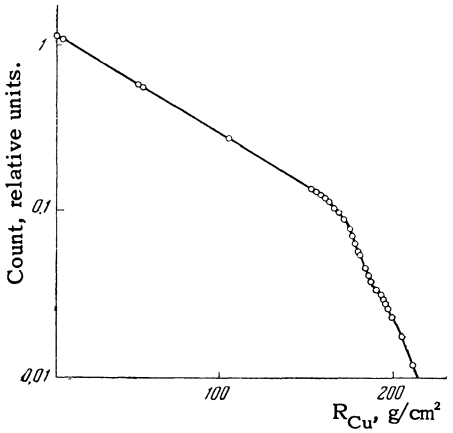

Fig. 1. Typical absorption curve (E_π = 307 Mev).

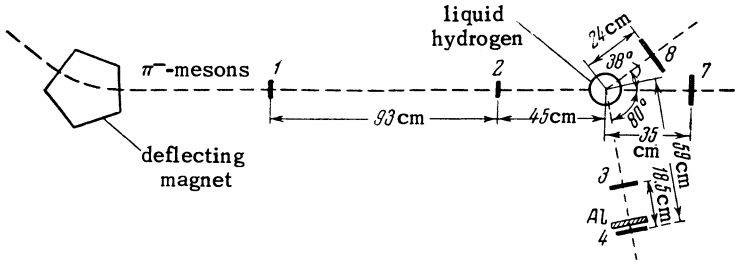

Fig. 2. Geometry of experiment.

are plexiglass containers filled with a solution of terphenyl in phenyl cyclohexane (3 grams per liter). Counters 5 and 6 are not shown on the diagram, for they have been used only in the study of elastic scattering. Counter 1 measures 6×6×1 cm, counters 3, 4, and 7 — 12.6×11.5×1 cm, and counter 8 — 16×17×1.5 cm. To reduce the background due to scattered mesons, counter 2 was made from a tolane crystal measuring 6×6×0.4 cm.

Counters 1, 2, 3, 7, and 8 were connected to photomultipliers by means of plexiglass light pipes. Counter 4 was connected to the photomultiplier with the aid of a hollow light pipe with polished aluminum walls. The need for using a hollow light pipe was dictated by the fact that plexiglass light pipes are sensitive to fast charged particles, although only with an effectiveness of approximately 5% (owing, apparently, to the Cerenkov radiation). The light-gathering effectiveness of such a light pipe is approximately one-half that of a plexiglass light pipe.

The photomultipliers were placed in a double magnetic shield for protection against the stray magnetic field of the synchrocyclotron magnet. Pulses from the photomultiplier were fed to an intermediate shaping cell (Fig. 3). Here the large

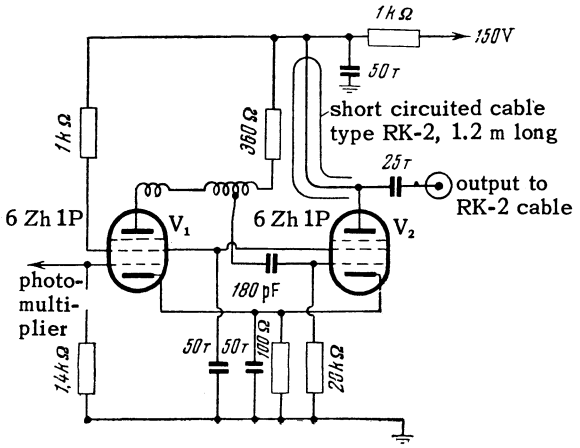

Fig. 3. Diagram of shaping cell (the letter T denotes capacitance in 1,000 μμF).

pulses were limited in amplitude in a simplified "semi-distributed" amplifier stage[4] with tube V_1, while the smaller ones were amplified by a factor of approximately two. The pulses were then shaped in duration by a short-circuited cable stub connected in the plate circuit of tube V_2, and were fed over high frequency coaxial cables approximately 80 m long to the coincidence circuits. The rise time of the pulse front at the output of the intermediate cell amounted to approximately 4×10^{-9}

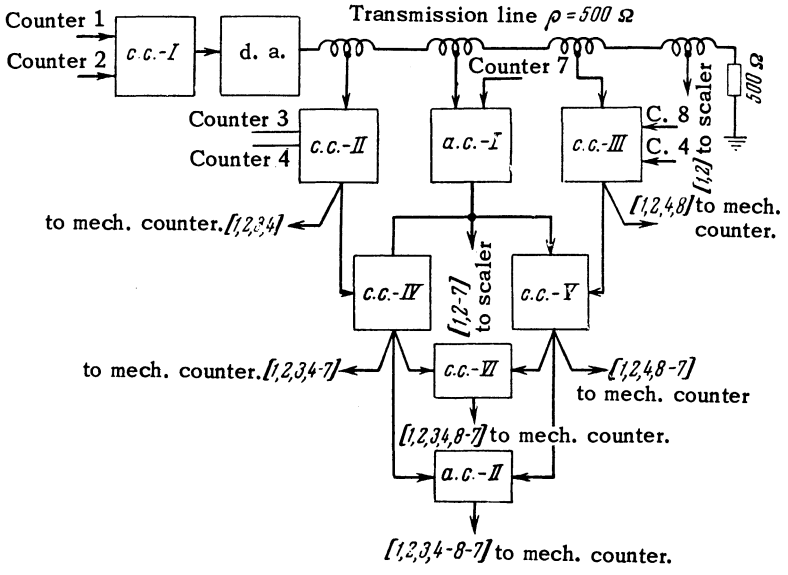

Fig. 4. Block diagram of electronic apparatus. c.c.-I — double coincidence circuit ($\tau \sim 1.2 \times 10^{-8}$ sec.); d.a. — distributed amplifier (f = 50-70 Mc); c.c.-II and c.c.-III — triple coincidence circuits ($\tau \sim 1.2 \times 10^{-8}$ sec.); a.c.-I — anticoincidence circuit ($\tau \sim 2.2 \times 10^{-8}$ sec.); c.c.-IV, c.c.-V, and c.c.-VI — double-coincidence circuits ($\tau \sim 5 \times 10^{-7}$ sec.); a.c.-II — anti-coincidence circuit ($\tau \sim 5 \times 10^{-7}$ sec.).

seconds in response to an input pulse with a front duration on the order of 10^{-9} seconds.

A block diagram of the electronic apparatus is shown in Fig. 4. The fast-coincidence circuits were designed with type DGTs germanium detectors. These circuits give resolution times up to 0.5×10^{-8} seconds at an approximate sensitivity of 0.5 v. The time characteristics of the FEU-19 photomultipliers, however, do not permit operation with a resolution time less than 10^{-8} seconds without loss in efficiency.

The double-coincidence circuit is shown in Fig. 5. It is similar in operating principle to the coincidence circuit described in Ref. 5. In the normal

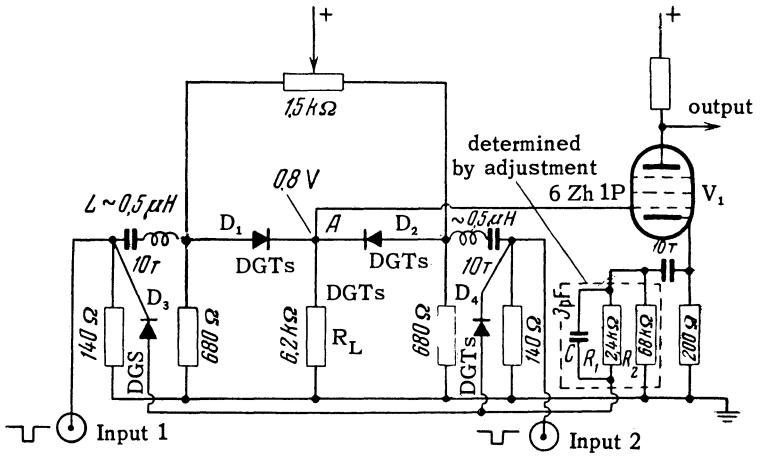

Fig. 5. Double coincidence circuit (monitor).

state, the potential of point A (output of the coincidence circuit) is determined by the currents flowing through detectors D_1 and D_2 and through load resistance R_L. The currents through the detectors are approximately equal in magnitude. If the pulse from the photomultiplier blocks only one of the detectors, for example D_1, the potential of point A changes insignificantly. This is due to the fact that the resistance of detector D_2 is small compared with the load R_L. By virtue of the nonlinearity of the voltage-current characteristic of the detector, doubling the current flowing through the detector produces a proportionately lesser voltage drop across the detector (by a factor 1.2 — 1.4). When detectors D_1 and D_2 are blocked simultaneously, the potential of point A tends to zero, and a negative pulse is produced at the output of the coincidence circuit. For satisfactory operation of the circuit it is necessary that the load resistance be many times greater than the high-frequency input impedance.

A distinguishing feature of the double-coincidence circuit employed here is the presence of a system to compensate for "single" pulses; this system comprises detectors D_3 and D_4 together with the RC network consisting of R_1, R_2, and C).

The pulse arriving at the input of the coincidence circuit is applied simultaneously through the compensation network to the cathode of tube V_1. The parameters of the compensation circuit are chosen to neutralize the pulse that appears at the output of the coincidence circuit whenever a pulse arrives from only one of the inputs. Thanks to the nonlinearity of the voltage-current characteristic of the detectors, the addition of the compensation network does not affect noticably the sensitivity of the coincidence circuit, for small pulses do not pass through detectors D_3 or D_4. The use of compensation has made it possible to reduce substantially the magnitude of the "single" pulses from the output of the double-coincidence circuit. This was important for clean operation (without false coincidences) of the triple-coincidence circuit.

The pulse from the output of the double-coincidence circuit is amplified by the distributed amplifier and applied to an artificial line with lumped constants, serving as a natural continuation of the anode line of the amplifier. The capacitances employed in this line are the inputs to four triple-coincidence circuits (of which only two are shown in the block diagram, Fig. 4), and the input to the fast anticoincidence circuit. This method of con-

necting the triple-coincidence circuit makes it possible to isolate the capacitances of the inputs of the individual circuits and to avoid trailing of the pulse from the output of the double-coincidence circuit. If the pulse applied to the input of the line has a front duration approximately 10^{-9} seconds, the rise time of the front of the line-output pulse is approximately 4×10^{-9} seconds.

The triple-coincidence circuit is shown in Fig. 6. It operates on the same principle as the double-coincidence circuit. No compensation circuit is provided. The relatively small pulses at the output of the triple-coincidence circuit, appearing when only one or two of the circuit detectors are blocked, are separated by means of a type DGS detector (D_4).

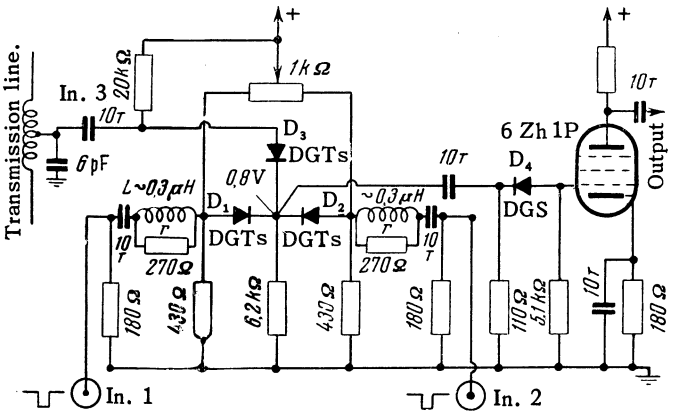

Fig. 6. Triple coincidence circuit (angle telescopes).

The fast anti-coincidence circuit is shown in Fig. 7. It comprises a double-coincidence circuit of the type described above, in which one of the detectors (D_1) is blocked. If a blocking pulse is applied to detector D_2, a pulse will also appear at the output of the anti-coincidence circuit. No pulse can appear at the output of the anti-coincidence circuit if D_2 receives a pulse from the output of the double-coincidence circuit, and simultaneously detector D_1 is unblocked by a positive pulse from tube V_1. The shaped pulses from the anti-coincidence circuit have an approximate duration of 2.2×10^{-8} seconds.

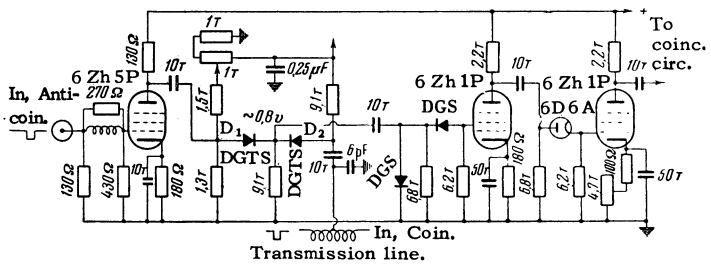

Fig. 7. Fast anticoincidence circuit.

The "slow" ($\tau \sim 5 \times 10^{-7}$ sec) vacuum-tube coincidence and anticoincidence circuits were operated by standard shaped pulses from the output of the "fast" circuits. The efficiencies of the coincidence and anticoincidence circuits were checked by arranging the corresponding counters in a single row in a beam of negative pions of reduced intensity. The efficiency of the coincidence circuit was close to 100%, that of the fast anti-coincidences not less than 97%, and that of the slow anticoincidence circuit not less than 99.9%

LIQUID HYDROGEN TARGET

The liquid hydrogen was placed in a vessel made of type PS-4 foamed styrol (density 0.04 g/cm^3). The vessel was attached to the individual blocks with BF-4 glue. The schematic construction of the foamed-styrol target is shown in Fig. 8. The target consists of an inner vessel 1, placed inside an outer vessel 2. The outgoing evaporating hydrogen flows over the walls of the vessels and cools them. To reduce the rate of evaporation of the liquid hydrogen, a jacket 3 of red copper 1 mm

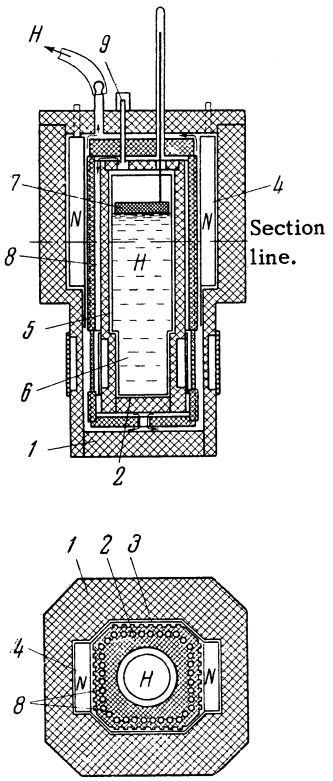

Fig. 8. Diagram of foamy polystyrol vessel for liquid hydrogen. 1 – outer vessel, 2 – inner vessel, 3 – cooling jacket of red copper 1 mm thick, 4 – pockets for liquid nitrogen, 5 – duraluminum cylinder, 6 – working portion of target, 7 – float, 8 – openings for evaporating hydrogen, 9 – filling tube.

thick is placed around the inner vessel and is cooled with liquid nitrogen poured into pockets 4. The walls of the vessel are made thinner at the place where the pion beam passes. The liquid hydrogen is poured into duraluminum cylinder 5. The wall thickness of this cylinder, in the working portion 6, is 0.1 mm. The diameter of the cylinder in the working portion is 11 cm. In the presence of liquid nitrogen in the nitrogen jacket, the rate of evaporation of liquid hydrogen is 0.7 l/hr. The hydrogen reserve (above the working portion) was 6 l. The amount of hydrogen in the target was controlled by means of a float level 7. The float and rod were made of foamed styrol. The wall thickness is 0.35 g/cm^2 across the beam path and 0.34 — 0.38 g/cm^2 in the target of the scattered pion. When the background was measured after evaporation of the liquid hydrogen, gaseous hydrogen was continuously blown through the empty target.

MEASUREMENTS AND CORRECTIONS

The experiment consisted of recording the charged mesons, created on hydrogen in processes (3) and (4), and traveling at an angle of 80° in the laboratory system. Such mesons produce four-fold coincidences in counters 1, 2, 3, and 4. Four-fold coincidences will be produced in counters 1, 2, 3, and 4 (and in greater quantity) also by mesons elastically scattered by hydrogen, along with the created mesons. To prevent counting of elastically-scattered mesons, the coincidences of counters 1, 2, 3, and 4 were connected for anticoincidence with counter 8 (Figs. 2 and 4), which was set at the angle of emergence of the recoil proton in elastic scattering (37.5 — 38°). Thus, the only four-fold coincidences of counters 1, 2, 3, and 4 recorded were those unaccompanied by the passage of a charged particle through counter 8. These will be called henceforth type Q coincidences.

Type Q coincidences can be produced by other than mesons formed on hydrogen. Such coincidences are possible also (a) when the recoil proton in process (1) is scattered by hydrogen and the target walls and does not enter counter 8, while the corresponding negative pion passes through the telescope comprising counters 3 and 4; (b) when the negative pions, previously elastically scattered by hydrogen at an angle other than 80° are secondarily scattered by hydrogen and by the target wall; (c) when the γ quanta from process (2) are converted in the walls of the target and in counter 3; (d) when the π^0 mesons from process (2) disintegrate (in 1.6% of the cases[6]) according to the scheme $\pi^0 \rightarrow \gamma + e^+ + e^-$ and the electrons enter into telescope 3, 4; (e) upon scattering of a negative pion with radiation ($\pi^- + p \rightarrow \pi^- + p + \gamma$).

Type Q coincidences are also recorded whenever the "slow" anticoincidence circuit does not operate for some reason. The correction for this ineffectiveness in the operation of the anticoincidence circuit does not exceed 0.1% of the elastic cross-section, amounting to approximately 1% of the mesons created by mesons at 307 Mev.

To determine the correction necessitated by (a) it is necessary to know the cross-section of process (1) at the given angle (coincidences of counters 1, 2, 3, 4, and 8). The coincidences of 1, 2, 3, 4, and 8 were recorded during the entire time of the measurement of Q. The number of recoil protons scattered in hydrogen and in the target walls was determined from the total cross-sections of the interaction between the nucleons and hydrogen and carbon.[7] Account was also taken of the multiple and single scattering of protons by the Coulomb field of the nuclei.

An exact determination of the contribution of the secondary scattering of negative pions is almost impossible. It was assumed as a first rough approximation that all the secondary scattered negative pions are isotropically distributed in space. The total number of the secondarily-scattered mesons was determined from the total cross-sections of the elastic scattering of negative pions by hydrogen and of the elastic and inelastic scattering by carbon.[8,9] The resultant number of secondarily-scattered mesons amounted to approximately 1.8% of the number of elastically scattered negative pions. It should be noted that the entire correction amounts to approximately 15% of the observed number of mesons created at 307 Mev, and is even less for higher energies.

To determine the corrections connected with effects (c) and (d), it is necessary to know the number of γ quanta that pass through counter 3. For this purpose, a lead converter 7.35 g/cm^2 thick was placed ahead of counter 3 to increase the efficiency of registration of γ quanta from process (2). Knowing the cross-sections for the conversion of γ quanta in hydrogen, carbon, and lead, it is possible to estimate the correction for conversion of γ quanta in counter 3 and in the target walls. It amounted to $4 \pm 1.5\%$ of the effect of lead.

No correction was introduced for pion scattering with radiation. Apparently, the cross-section of this process has a magnitude not more than 1% of the elastic scattering cross-section of negative pions by hydrogen.[10] At 307 Mev this may amount to approximately 10% of the observed creation of

mesons by mesons.

In addition to the above specific corrections, the "usual" corrections were made to account for the following effects: muon impurities in the beam (5 ± 1.5%), counting loss in the monitor (up to 6%) absorption of pions in the target walls and in the hydrogen, absorption of pions in counter 3, and decay of the pions.

To determine the background, not connected with the hydrogen, of mesons scattered in the target wall and in counters 2 and 7, and also the background of the random coincidences, measurements were made with an empty target. Measurements with delayed coincidences showed that the random coincidences were due predominantly to the passage of negative pions through counters 1 and 2, together with simultaneous random passage of some charged particles through counters 3 and 4. Counter 7, connected for anticoincidence with counters 1 and 2 (Figs. 2 and 4), served to reduce the background of random coincidences, so that type Q coincidences were recorded only when a negative pion from the beam was scattered in the target. This made it possible to reduce the background of random coincidences by a factor of approximately 20. The background of random coincidences was further reduced by placing an aluminum filter 5.4 g/cm^2 thick between counters 3 and 4. Thanks to the fact that the intensity of the synchrocyclotron did not vary about the mean level by more than 10% during the time of the measurement, the fluctuations of the background of random coincidences did not exceed ± 0.05 counts per 10^6 monitor counts. This amounted to approximately 7% of the total number of recorded mesons created at 307 Mev.

RESULTS AND CONCLUSION

The experimental quantities obtained at various energies and the corrections introduced into these quantities are listed in the table.

As expected, at a primary-beam energy of 250 Mev, the mesons created on hydrogen are not registered. This is connected with the fact that the created pion should have, under the conditions of our experiment, a kinetic energy in excess of 42 Mev in the laboratory system. Only then would it be registered with a nonzero probability. The high-energy registration threshold is due to a considerable extent to the aluminum filter placed between counters 3 and 4. The influence of the aluminum filter on the efficiency of registration of mesons of various energies was investigaged experimentally.

The presence of an energy threshold for pion registration causes a considerable portion of the mesons created on hydrogen to remain unregistered. To determine the fraction of registered mesons it is necessary to know the energy spectrum of the mesons created. Since no such information is available, it becomes necessary to make certain assumptions concerning the form of the spectrum. If one assumes that in the c.m.s. the energy spectrum is symmetrical about an energy equal to half the maximum energy of the created pions, it turns out that the registration efficiency (i.e., the fraction of registered mesons from the spectrum) does not depend too strongly on the form of the spectrum. Thus, the registration efficiency, for a beam of 307-Mev negative pions, amounts to 44.8, 43.4, and 42.7% for a rectangular, trapezoidal, and triangular energy spectrum

Production of Pions by Negative Pions on Hydrogen

Pion beam energy	Coincidence count 1, 2, 3, 4 – 7, 8 with hydrogen	Coincidence count 1, 2, 3, 4 – 7, 8 without hydrogen	Difference (mean, weighted)	Effect of lead (difference with and without hydrogen)	Effect 1, 2, 3, 4 – 7, 8 (difference with and without hydrogen)	Correction for γ quanta	Correction for elastic scattering	Number of type Q coincidences due to produced mesons, Q_{creat}	Recorded fraction of pions for trapezoidal energy spectrum, ε	Usual corrections, f	Differential cross-section for product of charged meson ($d\sigma/d\omega$), 10^5 c.m.s., × 10^{-27} cm^2/sterad	$2\sigma_{\pi^+} + 0.7\sigma_{\pi^-} = \frac{1}{4\pi}(d\sigma/d\omega)$ × 10^{-27} cm^2
250	8.97±0.75 11.86±0.6	7.43±0.52 9.99±0.53	1.73±0.6	23.2±2.1	9.83±0.47	1.31±0.33	0.32±0.15	0.1±0.7	approx. 0	—	—	—
307	10.17±0.32	8.33±0.26	1.84±0.41	14.7±1.7	8.5±0.32	0.81±0.2	0.26±0.13	0.77±0.48	0.44	0.96	0.099±0.062	1.24±0.78
333	10.27±0.37 16.4±0.9	7.50±0.36 14.1±0.8	2.70±0.48	14.3±1.6	8.44±0.32	0.79±0.2	0.25±0.13	1.66±0.54	0.57	0.95	0.166±0.054	2.09±0.68
370	10.89±0.63 11.51±0.59 10.86±0.55	6.60±0.44 6.90±0.53 7.37±0.55	4.13±0.45	11.2±1.9	8.01±0.32	0.62±0.2	0.24±0.12	3.27±0.51	0.67	0.92	0.287±0.047	3.61±0.59

respectively. The table gives the effectivenesses for a spectrum of trapezoidal form.

The differential cross-section for the production of a charged meson at an angle of 80° in the laboratory system was calculated from the formula

$$\left(\frac{d\sigma}{d\omega}\right)_{creat.} = (Q_{creat.}/N\omega f\varepsilon)\cdot 10^{-6}, \qquad (6)$$

where Q_{creat} is the number of type Q coincidences, obtained after subtracting the contribution of effects (a), (b), (c), and (d), per 10^6 monitor counts; $N = 0.443 \times 10^{-24}$ is the average number of hydrogen atoms per cm^2; $\omega = 0.0417$ steradians is the solid angle subtended by the telescope consisting of counters 3 and 4; ϵ is the registration efficiency of the produced pions, if the energy spectrum of this pion is trapezoidal in form; and f is a coefficient that accounts for the "usual" corrections. 80° in the laboratory system corresponds on the average to 105 — 107° in the c.m.s. The corresponding transfer coefficient for the differential cross-sections differs from unity, on the average, by not more than 1%.

The differential cross-sections, obtained at various energies, for the production of a charged meson at an angle of 80° in the laboratory system, or approximately 106° in the c.m.s., are given in Fig. 9. It is clear that the differential cross-section increases rapidly with the energy. At 370 Mev the measured cross-section amounts to approximately 60% of the differential elastic-scattering cross-section.

It is interesting to estimate, on the basis of the resultant differential cross-section, the approximate values of the total cross-section for the production of mesons by mesons on hydrogen. If it is assumed that in both processes (3) and (4) the angle of distribution of the mesons is isotropic and the mesons are not correlated, then the quantity $(d\sigma/d\omega)_{creat} \times 4\pi$ is the sum $2\sigma_{(3)} + 0.7\sigma_{(4)}$ of the total cross-sections of processes (3) and (4) (see table). The coefficient 2 in front of $\sigma_{(3)}$ is caused by the fact that two charged mesons are produced in process (3). The coefficient 0.74 in front of $\sigma_{(4)}$ is due to the fact that, as a rough estimate, approximately 30% of the recoil protons due to process (4) can enter into counter 8, correspondingly reducing the registration efficiency for the negative-pions from process (4).

The total cross-sections obtained under the above assumptions can be compared with recently-published theoretical results.[11,12] Reference 11 treats a charge-symmetrical pseudo-scalar interaction by the Tamm-Dancoff method, neglecting the amplitudes of all states that contain more than two mesons. According to this work, the contribution of meson-meson creation in the energy interval investigated by us is less than 1% of the elastic scattering. This is less than one tenth of our value. It must be noted that the Tamm-Dancoff method gives results that do not agree with experiment even for ordinary scattering of negative pions by protons.

In Ref. 12 the cross-sections of processes (3), (4), and (5) were calculated on the basis of the Chew and Low theory. The dependence of the sum $2\sigma_{(3)} + 0.7\sigma_{(4)}$ on the negative-pion energy, obtained on the basis of the data of that reference, is shown for comparison by the solid line of Fig. 9. From

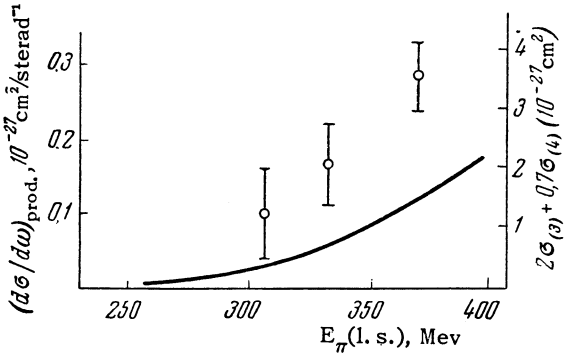

Fig. 9. Differential cross-sections for production of a charged pion at 80° in the laboratory system (106° in the c.m.s.) in processes (3) and (4) (left scale), and sum of total cross-sections $2\sigma_{(3)} + 0.7\sigma_{(4)}$ (right scale). The solid curve represents the sum $2\sigma_{(3)} + 0.7\sigma_{(4)}$, calculated on the basis of the Chew and Low theory.

the methodological point of view, it is interesting to note that there is no great discrepancy between our experimental data and those of Ref. 12.

The authors express their gratitude to Prof. B. M. Pontecorvo for constant attention and aid in the work.

[1] M. Blau and M. Caulton, Phys. Rev. **96**, 150 (1954). W. D. Walker and J. Steinhaber, Sixth Annual Rochester Conference on High-Energy Nuclear Physics, N. Y., 1956. Walker, Hushfar, and Shephard, Phys. Rev. **104**, 526 (1956).

[2] Ignatenko, Krivitskii, Mukhin, Pontecorvo, Reut, and Tarankanov, Атомная энергия (Atomic Energy) May, p 5 (1956).

[3] V. G. Zinov and S. M. Krenchenko, J. Exptl. Theoret. Phys. (U.S.S.R.) **33**, 335 (1957), Soviet Phys. JETP **6**, 260 (1958).

[4] S. T. Kalikhman, Радиотехника (Radio Engineering) June, p 52 (1953).

[5] W. C. Elmore, Rev. Sci. Instr. **21**, 649 (1950).

[6] Lindenfeld, Sachs, and Steinberger, Phys. Rev. **89**, 531 (1953).

[7] Gol' danskii, Liubimov, and Medvedev, Usp. Fiz. Nauk **48**, 531 (1952); **49**, 3 (1953).
[8] L. M. Barkov and B. A. Nikol' skii, Usp. Fiz. Nauk **61**, 341 (1957).
[9] Dzhelepov, Ivanov, Kozodaev, Osipenkov, Petrov, and Rusakov, J. Exptl. Theoret. Phys. (U.S.S.R.) **31**, 923 (1956), Soviet Phys. JETP **4**, 864 (1957).
[10] V. G. Solov' ev, J. Exptl. Theoret. Phys. (U.S.S.R.) **29**, 242 (1955), Soviet Phys. JETP **2**, 159 (1956).
[11] M. Nelkin, Phys. Rev. **104**, 1150 (1956).
[12] J. Franklin, Phys. Rev. **105**, 1101 (1957).

Translated by J. G. Adashko
61

SOVIET PHYSICS JETP VOLUME 34 (7), NUMBER 2 AUGUST, 1958

DISTRIBUTION OF MAGNETIC INDUCTION IN THE INTERMEDIATE STATE OF A CURRENT-CARRYING SUPERCONDUCTOR

B. V. MAKEI

Institute of Physics of the Polish Academy of Science, Wroclaw

Submitted to JETP editor July 25, 1957

J. Exptl. Theoret. Phys. (U.S.S.R.) **34**, 312-315 (February, 1958)

The distribution of the magnetic field in a slot cut out in the middle part of a tin cylinder carrying a current was measured by the bismuth probe method. The slot was located in a diametral plane of the cylinder. The results obtained are compared with the London and Landau phenomenological theory of the distribution of current density in the intermediate state of a cylindrical superconductor. The existence of a core of intermediate state in a superconducting wire carrying a current above critical is directly demonstrated by the experiments.

INVESTIGATIONS of the breakdown of superconductivity by current are basically devoted to the study of the change of electrical resistivity of a specimen in dependence on temperature and the electric current flowing through it.[1-4] As it appears to us, measurement of the magnetic induction inside a specimen through which an electric current is flowing can also give valuable information on the intermediate state of a superconductor.

In the present work we report the results of measurements of the magnetic induction inside a current-carrying tin specimen 4 mm in diameter and 56 mm long. A 0.2 × 3.5 mm rectangular slot was cut in the central portion of the cylinder and situated in a diametral plane (with the long side of the slot parallel to the axis of the specimen). The magnetic field was measured by means of a bismuth probe (Fig. 1), such as is used in the study of the microstructure of magnetic fields.[5,6] The

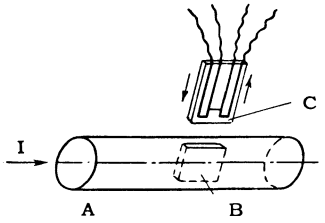

FIG. 1. Diagram of the experiment. A – specimen, B – slot, C – platelet with probe.

probe was a straight segment of bismuth wire 1.5 mm long and 20 μ in diameter, soldered to thin copper strips which served as potential and current leads. To protect the probe against mechanical disturbances, the copper strips were glued between rectangular mica platelets. The probe was moved along the slot (perpendicular to the axis of the specimen) by means of a mechanism with a micrometer screw. The current was fed to the specimen under test by copper tubes tinned with

up the crystals as infinitely long unidimensional or two-dimensional atom complexes, bound together by "small" forces of one nature, whereas in the complex itself the atoms are bound by "big" forces of another nature.

6. The difference between the typical molecular crystals (e.g., the CH_4 or C_6H_6 crystals) and the heteropolar molecular crystals (such as the NaCl, $HgCl_2$ or PbS crystals) lies: (1) in the degree of molecularity β; (2) in the nature of the forces in the molecules; (3) in the nature of intermolecular forces. The quantity β is defined as the ratio of the intramolecular energy $U^a \cong D$ (D is the energy of dissociation of the diatomic molecule into ions) to the intermolecular energy U^e per bond. For the substances for which β is given below, it is possible to take $U^e \approx 2S/l$. Example:

$\beta = 300(CH_4)$, $200(HCl)$, $22(HgCl_2)$, $10(NaCl)$ taking $l = 12$ in all four cases.

Translated by I. Polidi
334

ERRATA

Volume 5

Page	Line	Reads	Should Read
1043	Eq. (4)		$W = y^2 a_{14}^2 \sin 2\phi/2\rho\,(a_{11}a_{44} - \alpha_{14}^2 \sin^2 3\phi)$ The coefficient k_2 equals $0.185 \times 10^{-3}\,cm^{-1}$.
1044	3 from bottom (l.h.)	$\Delta y = 2.87 \times 10^{-3}$ cm	$\Delta y = 3.18 \times 10^{-3}$ cm
	4 from top (r.h.)	$\Delta\vartheta_\Sigma = 7.2 \times 10^{-5}$ radians	$\Delta\vartheta_\Sigma = 5.9 \times 10^{-5}$ radians

Volume 6

1090	4 and 5 from top	2—(d, 3n); and of the I_{53}^{127} cross section, 3—(d, 2n); 4—(d, 3n)	2—(d, 3n) on I_{53}^{127} and 3—(d, 3n); 4—(d, 3n) on Bi_{83}^{209}
1091	6 from bottom expression for determinant C(y)	ρ, γp, h, $1/\rho$	ρy_2, $\gamma p y_2$, $h y_2$, y_2/ρ
1094	7 from bottom	For $\gamma = 5/3$, μ has . . .	Here μ has . . .

Volume 7

55	16 from bottom	Correct submittal date is April 5, 1957	
169	17 from bottom	Delete "Joint Institute for Nuclear Research"	
215	Table	Add: Note. Columns 2—9 give the number of counts per 10^6 monitor counts	
215	Table, column headings	1, 2, 3, 4-7, 8	1, 2, 3, 4, 8-7
312	Eq. (8)	. . . $(1 \pm \mu/2M)^2$	. . . $(1 \mp \mu/2M)^2$
313	2, r.h. col.	$\alpha_{33} = 0.235$	$a_{33} = 0.235$
692	Eq. (5)	$m_B/M_B = \ldots \mp [1 + \ldots]$	$m_B/M_B = \mp [1 + \ldots]$
461	Title	. . . Elastically Conducting	. . . Electrically Conducting